Communications on Applied Nonlinear Analysis
ISSN: 1074-133X
Vol 32 No. 3s (2025)

Border Detection of Skin Cancer Cells over Fractal Dimension Analysis and Image Processing Techniques

[1]P.Tharaniya, [2]R.Ambrose Prabhu, [3]V.Sumathi [4]R.Rajalakshmi, [5]R.Malarkodi, [6]R.Geethanjaliyadav

[1,2,3]Department of Mathematics, Rajalakshmi Instititue of Technology, Chennai, India,
[1]tharamanisharmi@gmail.com, [2]bennyamb0457@gmail.com, [4]vsumathigeerthana83@gmail.com
[4]Assistant Professor, Department of Mathematics,Panimalar Engineering College, Chennai, rajimat2020@gmail.com,
[5]Department of Mathematics, St.Joseph's college of Engineering and Technology, Thanjavur, India,
r.malarkodi26@gmail.com
[6]Department of Mathematics, Rajalakshmi Instititue of Technology, Chennai, India, rvgeetha20@gmail.com

Article History:

Received: *19-09-2024*

Revised: *03-11-2024*

Accepted: *16-11-2024*

Abstract:
Fractal dimension analysis is a novel technique that uses the self-similarity qualities of fractals to identify irregular forms, such as those prevalent in diseased tissues, in order to detect the borders of skin cancer cells. Acquire detailed pictures of skin tissue samples that have cancer cells in them. A variety of imaging methods, including microscopy and medical imaging tools like MRIs and CT scans, can be used for this. Determine the image's fractal dimension by applying suitable methods, like the fractal signature method or box-counting. A geometric shape's complexity is measured by its fractal dimension, and because malignant cells have uneven edges, they typically show higher complexity. To increase the border recognition process' accuracy, clean the photos to get rid of noise and boost contrast. Here, methods such as morphological procedures, histogram equalization, and median filtering can be used. To increase the border detection system's accuracy and resilience, fine-tune the parameters and algorithms in light of the validation results. A reliable approach for identifying the borders of skin cancer cells can be created by fusing fractal dimension analysis with image processing methods. This will help with early detection and therapy planning. Based on the fractal dimension, choose an appropriate threshold value to divide the image into zones of interest. This stage aids in the malignant cells' separation from the surrounding tissue.

Keywords: Fractal Dimension Analysis, Skin Cancer Cells, Border Detection, Image Processing, Medical Imaging

MSC Classification Key: 28A80, 62P10, 65D18, 92C50, 68U10.

1. Introduction

The largest organ in the body is frequently referred to as the skin. It keeps water and other bodily fluids inside the body, aids in controlling body temperature, produces vitamin D, and carries out a number of other intricate tasks that safeguard individuals. Of all cancers, skin cancer is the most prevalent. Fifty percent of all cancer cases are caused by it. It is a skin cancerous growth that has a variety of reasons. Usually, skin cancer starts in the epidermis, which is the skin's outermost layer. Therefore, Tumor is typically easily seen. Because of this, the majority of skin cancers can be found early on. The most common cause of this malignancy is prolonged skin exposure to UV (ultra violet) radiation.

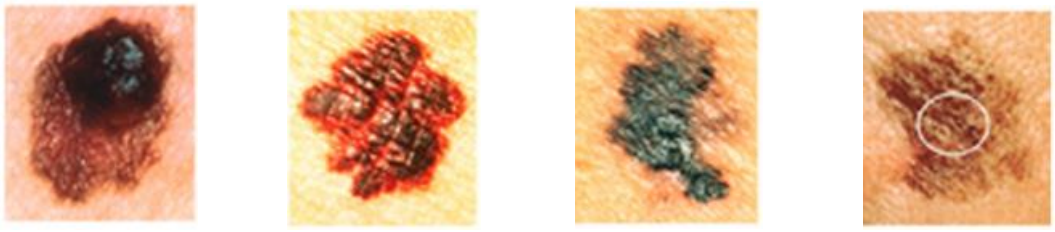

A: Asymmetry B: Border irregularity C:Color D:Diameter: ¼ inch or 6mm

Fig. 1.1: Diagnose Skin Cancer

Certain physical characteristics, including as shape, edge, color, and surface texture, can be used to identify skin cancer. It found that the most important diagnostic criteria was the irregularity of the border of the pigmented skin lesions. According to research by Morris Smith, one of the main vocabulary words used in medical textbooks to characterize the border of malignant melanoma is irregularity. A stands for asymmetry, B for border, C for color, and D for diameter. The ABCD checklist (Fig. 1.1) can be used to diagnose skin cancer border irregularity.

The Box-Counting Method (D_B) can be used to determine the size of the cell, and the Sausage Method (D_S) can be used to determine how invasive the malignancy is. Fractal geometry offers techniques for defining complexity, which can be utilized to qualify morphologies in image analysis content that are currently only qualitatively evaluable or that are thought to be random or irregular.

Here, we have used the Sausage Method (D_S) to highlight the invasiveness, and the Box Counting Method (D_B), which is found for a small number of samples, can be used to determine the overall dimension. The cancer image is handled as if it were two-dimensional, with coordinates defined as *(x, y).* The picture pixel size in the tissue is represented by s, and the (x, y) coordinates are then divided into grids that measure. When the minimum and maximum binary image levels in the $(i,j)^{th}$ grid are *(k-1)* and l, respectively, and fall into the and boxes, the contribution of in the $(i,j)^{th}$ grid is defined as

$$n_r(i,j) = l - k + 1.$$

The formula for calculating box counting dimension is calculated as

$$\dim_B F = \lim_{\delta \to 0} - \frac{\log N_\delta(F)}{\log \delta},$$

using least-squares linear regression to estimate the box-counting dimension yields the line's slope.

If the least and highest binary image levels in the $(i,j)^{th}$ grid, respectively, are *(k-1)* and l, and they fit into the boxes, $N(r)$ is described as the total of the contributions made by each grid present in a window of the picture.

$$N(r) = \sum_{i,j} n_r(i,j).$$

The slope of the line that best fits points $(\log\left(\frac{1}{r}\right), \log N(r))$ can be used to estimate the fractal dimension if $N(r)$ is calculated for various amounts of scaling r.

Step 1: Regular meshes with a mesh size of 'r' are created from the image.
Step 2: Determine $N(r)$ how many square boxes cross the image.

Step 3: $N(r)$ depends on r

Step 4: We count the corresponding number $N(r)$ after repeating for a number of size values.

Step 5: Form the slope D by plotting log $(N(r))$ against log $\left(\frac{1}{r}\right)$

The fractal's dimensions or level of complexity are indicated in Step 5. Finally, the least squares approach is used to fit a straight line to the plotted points in the diagram. The fractal dimension was estimated using a linear regression equation

$$\log\big(N(r)\big) = \log k + D \log\left(\frac{1}{r}\right),\ \text{k is constant,}$$

Where D denotes the dimension of the fractal. Numerous patients have had the aforementioned technique used to determine the size of their cancer cells. The above algorithm has been programmed and run in MATLAB.

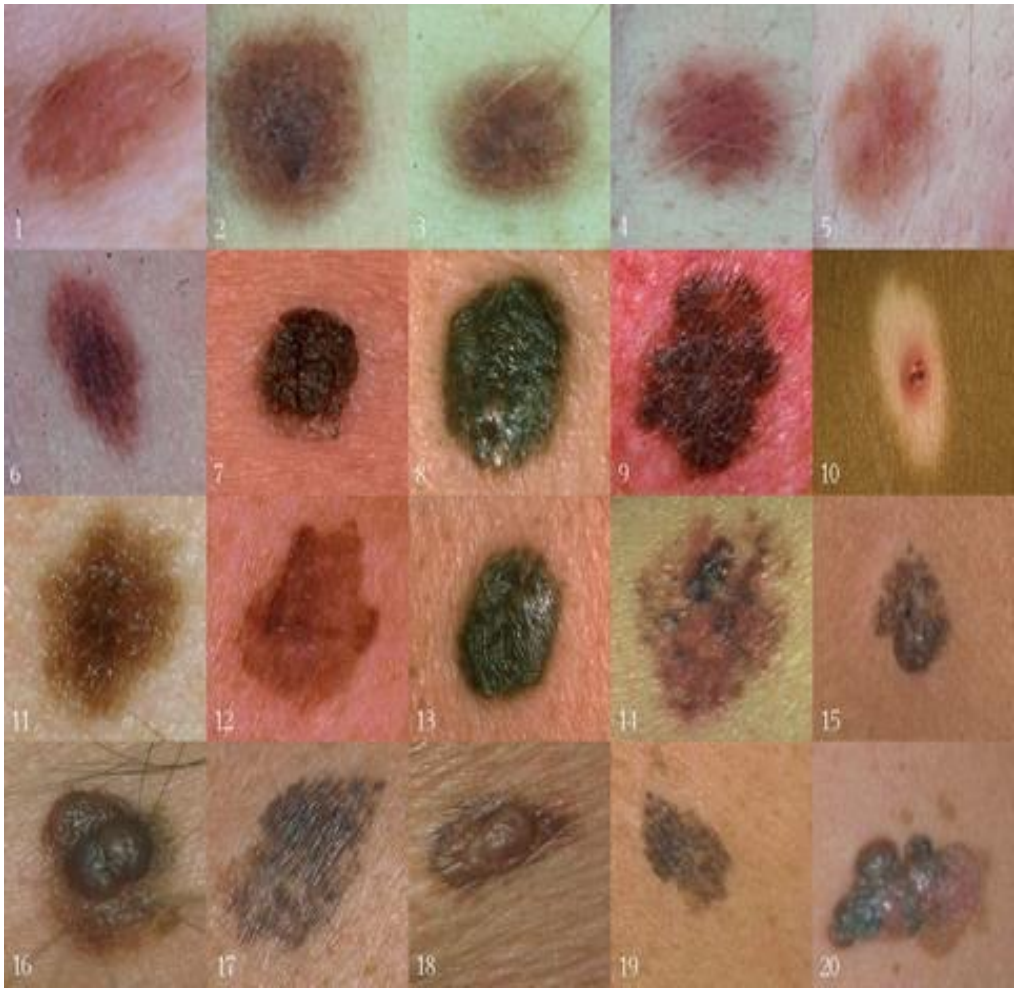

Fig. 1.2: Twenty Original Images of skin lesions

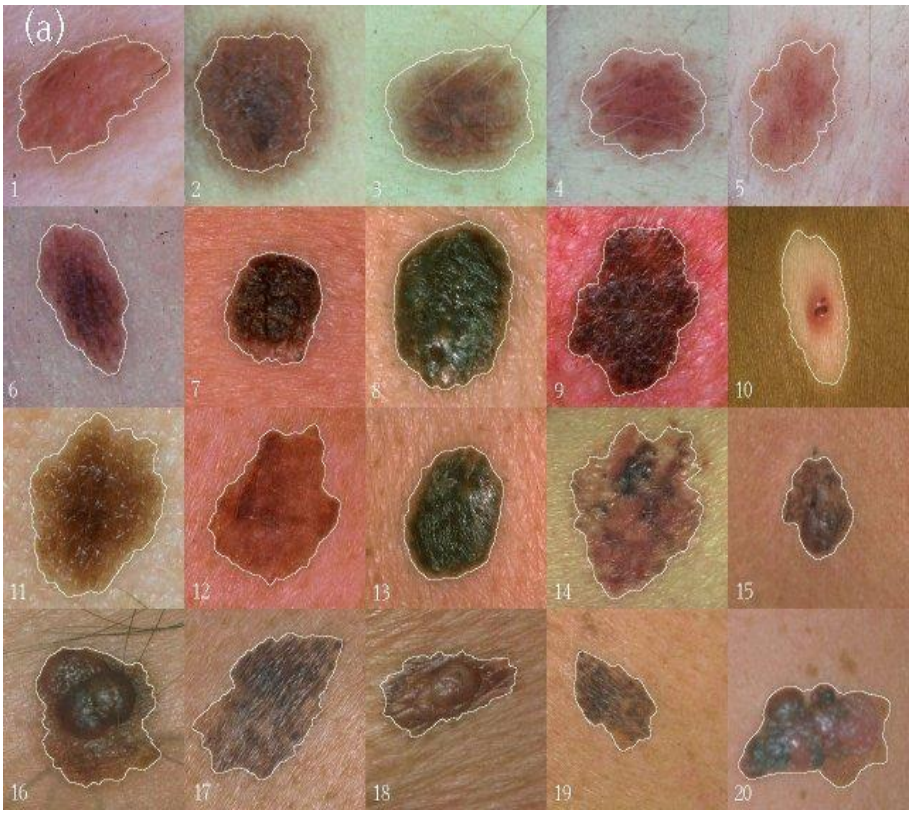

Fig. 1.3: Dermatologist Image of skin lesions

1.1.1 Literature Review

Ahmed [1] addresses the application of fractal geometry to the study and identification of cancer in a 1993 publication in the International Journal of Theoretical Physics. The study investigates the potential applications of fractal geometry—which deals with intricate patterns that display self-similarity at various scales—to biological tissues. This idea could be applied to medical imaging to improve cancer detection and diagnosis, offering a non-invasive way to spot cancers.

M. A. Aon and S.Cortassa [2] investigates the application of fractal analysis in comprehending and identifying cancer through cellular architecture in their 1994 paper published in FEBS Letters. Aon and Cortassa specifically look at how anomalies linked to cancer can be found by using the fractal character of cellular structures. Fractal analysis may be used to detect cancer since malignant cells frequently have distinct fractal dimensions from healthy cells.

M. Battaglia-Parodi and D. D. Giusto [3] examines the use of fractal analysis in the diagnosis of eye-related diseases and makes comparisons with its application in the detection of skin cancer. They contrast the usefulness and usability of fractal analysis in skin cancer research with its application in ophthalmology diagnosis.

Block. A [4] use of fractal geometry in biological systems is examined in this article, with a special emphasis on its uses in cancer research. Researchers may be able to detect and measure these anomalies in tissue samples by using fractal analysis, which could provide a novel method for the identification and diagnosis of cancer. Buckland-Wright. J. C., et. al [5] examines the application of fractal analysis to bone structure and its link with malignant alterations. The main focus of the

research is on how to quantify the fractal dimension of bone formations and how variations in these dimensions may be related to cancer.

Cross [6] uses of fractal dimension as a diagnostic technique to distinguish between tissues that are benign and those that are cancerous is covered in this article. In a study that they describe, the scientists used fractal analysis to analyze a variety of tissue samples and discovered that cancerous tissues frequently have larger fractal dimensions than benign ones.

Dubuc. B [7] presents a brand-new method for studying cancer that makes use of fractal analysis. They investigate the use of fractal geometry in microscopic imaging and its relevance to the research of malignant tissues. The authors draw attention to how this strategy may further our knowledge of how cancer progresses and lead to better detection methods.

Giusto, D. D [8] uses of fractal dimension analysis to the study of pathological disorders is the main topic of this article, which includes a case study specifically on skin cancer. The authors compare their findings to other clinical states and investigate the potential utility of the fractal dimension of skin tissue in identifying malignant alterations. Landini. G [9] have been applied to the study of diverse tissues, including cancer-affected tissues.An extensive summary of the use of fractal geometry in biological tissue analysis is given in this review paper.

MacAulay, C [12] explain about how to fractal dimensions are used to quantitatively analyze cell architecture with an emphasis on cancer diagnosis. The authors explain how the complexity of cell structures can be quantified in cytology and histology by using fractal analysis. This approach's theoretical and practical elements are presented in the study, emphasizing its potential to increase the precision of cancer diagnosis.

Post. U [13] investigates biological systems' fractal patterns and how they relate to cancer diagnosis. The writers talk on how fractals' erratic and self-similar patterns can be seen in a variety of biological tissues, including cancerous ones. The study offers a theoretical examination of these patterns along with suggestions for applying fractal geometry to the identification of malignant tissue alterations.

Rogers. G. W [14] focuses on the cell-by-cell cancer detection utilizing fractal dimension analysis. The authors present a technique for evaluating the complexity of individual cells using fractal geometry and identifying malignant alterations. The study provides experimental data showing how well this method distinguishes between benign and malignant cells.

Ryser, M. D [15] investigates the modeling of cancer cell invasion and proliferation using fractal dimension. The authors describe a mathematical model that mimics the behavior of cancer cells as they proliferate and infiltrate neighboring tissues by utilizing fractal geometry. The work emphasizes the diagnostic and therapeutic implications of fractal analysis, implying that a better knowledge of the fractal patterns of malignant growth may result in more potent therapy approaches.

Sadana, A [16] use fractal geometry in conjunction with biosensing technology to improve cancer detection techniques is covered in this article. This strategy may result in earlier and more sensitive and accurate cancer detection, enhancing diagnostic capacity and treatment results.

Traverso.S [18] use of fractal dimension analysis to identify malignant cells is presented in this article.. This suggests that fractal analysis may be a useful method for cellular cancer identification.

The study also explores how this approach might be used in clinical settings to improve the precision and dependability of cancer diagnosis.

1.2 Research Gap

La Brun [10] introduced in this article as a novel approach to cancer screening. The authors address the possibility of identifying and analyzing malignant tissues using fractal dimensions, and they suggest that this method could result in notable improvements in diagnostic precision. Liebovitch, L. L [11] tissues is examined the application of fractal analysis to the study of malignant in this article. With an emphasis on using fractal dimensions to distinguish between healthy and malignant tissues, the authors provide a mathematical framework for employing fractal geometry to analyze tissue architectures. We introduce the image fractal dimension method for distinguishing cancer cells. We apply new methods such as fractal signature method and box-counting method for determining the image's fractal dimension.

1.3 Notations

D_B : Box-Counting Method

D_S : Sausage Method

MM : Malignant Melanoma

HMM : Hidden Markov Model

Dim $_B$ F: box counting dimension

p : Probability

f(n) : function

N : Natural numbers

R : Real numbers

d(i) : Radial distance

2 Percolation Model

In the process of the disease spreading throughout the organ, a single percolation cluster (cancer cell) is produced. Each site in a square lattice represents a person who has a probability of *(p)* of infection and a probability of *(1-p)* of immunity. The person at the centre of the lattice (cell) is infected at initial time $t = 0$. We now assume that all non-immune nearby neighbour sites become infected by this infected site within a single unit of time. These infected sites will spread to all of their nearby, non-immune neighbour sites in the second unit of time, and so forth. This means that all of the non-immune spots in the square grid surrounding the cells are infected after t time steps, or the longest possible path between the infected sites and the cell is $l \cong t$.

2.1 Algorithm

Step 1: Begin at the origin, which is the centre of the empty site (square lattice).
Step 2: The closest neighbouring sites are either blocked with probability (p) or occupied with probability (p) from the origin.

Step 3: The empty nearest neighbour sites are blocked with probability and proceed with probability (p) as in Step 2. The aforementioned technique is very helpful for researching the composition and characteristics of a single percolation cluster.

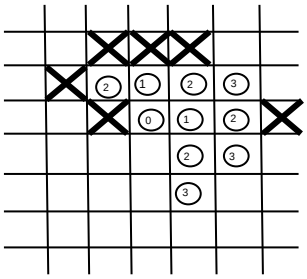

Fig. 1.4: First four steps for the percolation model

3 Boundary Descriptors

When representing an item with an irregular shape, the border direction is a better choice. Relative position or direction is indicated by consecutive points on a shape's boundary. Applying the Theorem of Maximum Modulus Let *f(z)* be analytic and non-constant in the interior of D and continuous in a closed, bounded area D. Then, and never within D, |*f(z)*| reaches its maximum value on D's perimeter. Cell growth is based on the aforementioned theorem. Inside the tissue, cell growth is erratic and non-constant, but it is continuous outside of a closed, bounded area. The cell can then reach its maximum on the tissue's periphery and never within. Thus, we may determine the maximal boundary of skin cancer (MM) based on the aforementioned theorem. Cell compactness in tissue and the Box Counting Method can both be used to demonstrate this. Compactness $\left(\frac{Perimeter^2}{Area}\right)$ is a dimensionless number that is minimal for a region with an irregular shape. This straightforward test determines how aggressive the skin cancer is.

3.1 Radial Distance Measure

Perimeter is an important feature of a cell. Contour based features which ignore the interior of a shape, depend on finding the perimeter or boundary points of the cell. This perimeter is used for the parametric boundary representation,

$$T = \int \sqrt{x^2(t) + y^2(t)}\, dt. \qquad (1.1)$$

Minkowski-Bouligand dimension is defined as if A is a bounded set of Euclidean space, then $A(\varepsilon)$ is the set of all points at a distance less than ε from A, and the "thickened" set $A(\varepsilon)$ is also called Minkowski Sausage. It is the union of all balls of radius ε centered on A. Denoting the volume by V, we get the Minkowski-Bouligand dimension is

$$D_M = \lim_{\in \to 0} \left(3 - \frac{\log V(A(\epsilon))}{\log \varepsilon}\right). \qquad (1.2)$$

By the aid of Sausage Method or Boundary Dilation Method which is very closely related to the Minkowski Dimension. The images were dilated with circles of increasing diameter. As an approximation for a circle boxes with pixel sizes of $1\times1,\ 3\times3,\ 5\times5,...,17\times17$ were again used.

The corresponding approximated radius *r* in pixels was calculated by

$$r = \left(\frac{A}{\pi}\right)^{1/2} \quad (1.3)$$

where A denotes the area in pixel.

The slope k_S of the regression line of the double logarithmic plot of the counted pixels with respect to the radii provides

$$D_s = 2 - k_s \quad (1.4)$$

The estimated fractal capacity dimension is D_S. In this method, the diameter of the cell can be calculated. The quantitative parameters such as Area, Perimeter, Form factor and Invaslog can be found out using Sausage method (Fig. 1.2 & 1.3).

$$Formfactor = \frac{4\pi\, Area}{Perimeter^2} \quad (1.5)$$

$$Invas\log = -\log(formfactor) \quad (1.6)$$

The value of $Invas\, log$ has been specially proven to be a strong quantitative measure of the invasiveness of skin cancer. Radial distance is the distance from the centre of the mass to the perimeter point (x_i, y_i) So the radial distance is defined as

$$d(i) = \sqrt{(x_i - \bar{x})^2 + (y_i - \bar{y})^2}, i = 0,1,2 \ldots . N - 1. \quad (1.7)$$

Here $d(i)$ is a vector obtained by the distance measure of the boundary pixels.

A normalized vector $r(i)$ is obtained by dividing $d(i)$ by the maximum value of $d(i)$.

4. Statistical Analysis

The reliability of statistical analysis results is influenced by the quantity of samples per statistical group, which supports the final conclusions. This number is constrained, on the one hand, by the experiment's real-time nature and the researchers' practical capacity to manage a high number of samples. However, since the variance is inversely related to the square root of the number of samples examined, the number must be suitably high. Therefore, for these trials and the statistical analysis of the data, more than 20 samples were selected. The probability distribution of the cells inside each tissue was used to calculate the fractal dimension for that tissue. The nonlinear regression equation $y = a\, x^b$, where y is the number of cells within a square of the grid with a given radius x, an is the scaling coefficient, and b is the fractal dimension, was fitted to numerical experimental data.

4.1 Results

Estimating the fractal dimension D with two different methods (D_B & D_S) for the twenty samples. The large set of image sequences yielded a large amount of information, if *D* is the dynamic behavior of the Cancer Invasion, Percolation Model.

Table 1.1. Data analysis of a typical Image using Box-Counting Method (Original Image)

Scaling	Original Image I					
	Area	**Perimeter**	**Total Area**	**Form Factor**	**Invaslog**	**Dimension D_b**
2	4631	742	5373	0.106	0.975	
3	1945	604	2549	0.067	1.174	
4	1046	426	1472	0.072	1.143	
5	635	352.6	987.6	0.064	1.194	
6	423	286	709	0.065	1.187	1.33
7	300	241	541	0.65	1.187	
8	220	190	410	0.77	1.114	
9	162	177	339	0.065	1.187	
10	128	15.6	278.6	0.071	1.149	
Scaling	**Original Image II**					
	Area	**Perimeter**	**Total Area**	**Form Factor**	**Invaslog**	**Dimension D_b**
2	6783	488	7271	0.358	0.446	
3	2923	389	3312	0.243	0.614	
4	1612	293	1905	0.235	0.629	
5	1009	231.6	1240.6	0.236	0.627	
6	683	194.83	877.83	0.226	0.646	1.21
7	490	170	660	0.213	0.672	
8	376	137	513	0.252	0.599	
9	283	128.89	411.8	0.214	0.670	
10	229	107.3	336.3	0.250	0.602	

Table 1.2. Data analysis of Atypical Image using Box-Counting Method (Dermatologist Image-1)

Scaling	Dermatologist Image I					
	Area	**Perimeter**	**Total Area**	**Form Factor**	**Invaslog**	**Dimension D_b**
2	1180	375	1555	0.105	0.979	
3	480	261	741	0.089	1.051	
4	242	189	431	0.085	1.071	
5	142	152	294	0.077	1.114	
6	92	115	207	0.087	1.060	1.67
7	67	86	153	0.114	0.944	
8	46	78	124	0.095	1.022	
9	35	61	96	0.118	0.928	
10	25	59	84	0.090	1.046	
Scaling	**Dermatologist Image II**					
	Area	**Perimeter**	**Total Area**	**Form Factor**	**Invaslog**	**Dimension D_b**
2	1757	277	2034	0.289	0.541	
3	738	197	935	0.239	0.622	1.52
4	400	140	540	0.256	0.592	

5	245	108	353	0.264	0.578	
6	165	88	253	0.268	0.572	
7	118	71	189	0.294	0.532	
8	88	59	147	0.318	0.498	
9	68	46	114	0.404	0.394	
10	53	40	93	0.416	0.381	

Table 1.3: Data analysis of Atypical Image using Sausage Method for Image I & II

Scaling	**Original Image I**				**Dermatologist Image I**			
	Area	**Radius**	K_s	$D_s = 2 - K_s$	**Area**	**Radius**	K_s	$D_s = 2 - K_s$
2	1945	24.882			480	12.361		
3	635	14.217			142	6.723		
5	300	9.772	0.67		67	4.618		
7	162	7.181		1.33	35	3.338	0.33	1.67
9	103	5.726			21	2.585		
11	69	4.687			11	1.871		
13	47	3.868			7	1.493		
15	36	3.385			7	1.493		
Scaling	**Original Image II**				**Dermatologist Image II**			
	Area	**Radius**	K_s	$D_s = 2 - K_s$	**Area**	**Radius**	K_s	$D_s = 2 - K_s$
3	2923	30.503			738	15.327		
5	1009	17.921			245	8.831		
7	490	12.489			118	6.129		
9	283	9.491	0.79	1.21	68	4.652	0.48	1.52
11	185	7.674			42	3.656		
13	127	6.358			28	2.985		
15	92	5.412			19	2.459		
17	68	4.652			14	2.111		

Benign Image : The given Table 1.1,1.2 and 1.3 shows the data produced by way of Box Counting Method and Sausage Method respectively.

Table 1.4: Data analysis of Benign Image using Box-Counting Method (Original Image)

Scaling	**Original Image I**					
	Area	**Perimeter**	**Total Area**	**Form factor**	**Invaslog**	**Dimension D_b**
2	4693	1982	6675	0.015	1.824	
3	1813.7	1442.33	3256	0.011	1.959	
4	940.4	961.75	1902.13	0.013	1.886	
5	563	702	1265	0.014	1.854	
6	373	513.17	886.17	0.018	1.745	1.34
7	262.4	396.86	659.29	0.021	1.678	

8	189.5	314.63	504.09	0.024	1.620	
9	150	249.52	399.52	0.030	1.523	
10	115	210.5	325.5	0.033	1.481	
Scaling	**Original Image II**					
	Area	**Perimeter**	**Total Area**	**Form factor**	**Invaslog**	**Dimension D_b**
2	6582	962	7544	0.089	1.051	
3	2730.67	780.67	3511	0.056	1.252	
4	1474	559	2033	0.059	1.229	
5	879.60	447.60	1327.20	0.055	1.260	
6	575.67	363.33	939	0.055	1.260	1.31
7	392.58	314.58	707.14	0.050	1.301	
8	293.5	251	544.5	0.059	1.229	
9	207.56	231.89	439.44	0.049	1.310	
10	159.2	200.4	359.6	0.050	1.301	

Table 1.5. Data analysis of Benign Image using Box-Counting Method (Dermatologist Image)

Scaling	**Dermatologist Image I**					
	Area	**Perimeter**	**Total area**	**Form factor**	**Invaslog**	**Dimension D_b**
2	1053	415	1468	0.077	1.114	
3	406	277	683	0.066	1.181	
4	208	185	393	0.076	1.119	
5	123	134	257	0.086	1.066	
6	86	104	190	0.100	1	1.67
7	59	81	140	0.113	0.947	
8	43	62	105	0.141	0.851	
9	32	48	80	0.175	0.757	
10	24	44	68	0.156	0.807	
Scaling	**Dermatologist Image II**					
	Area	**Perimeter**	**Total area**	**Form factor**	**Invaslog**	**Dimension D_b**
2	1653	384	2037	0.141	0.851	
3	659	292	951	0.097	1.013	
4	344	206	550	0.102	0.991	
5	203	160	363	0.100	1	
6	130	130	260	0.097	1.013	1.67
7	86	108	194	0.093	1.032	
8	61	88	149	0.099	1.004	
9	43	80	123	0.084	1.076	
10	31	72	103	0.075	1.125	

Table 1.6. Data analysis of Benign Image using Sausage Method for Image I & II

Scaling	Original Image I				Dermatologist Image I			
	Area	**Radius**	K_s	$D_s = 2 - K_s$	**Area**	**Radius**	K_s	$D_s = 2 - K_s$
3	1813.67	24.027			406	11.368		
5	563	13.387			123	6.257		
7	262.43	9.140			59	4.334		
9	150	6.910	0.66	1.34	32	3.192	0.32	1.68
11	91.37	5.393			21	2.585		
13	64	4.514			13	2.034		
15	46	3.827			8	1.596		
17	37	3.432			5	1.262		
Scaling	**Original Image II**				**Dermatologist Image II**			
	Area	**Radius**	K_s	$D_s = 2 - K_s$	**Area**	**Radius**	K_s	$D_s = 2 - K_s$
3	2730.67	29.48			659	14.48		
5	879.60	16.73			203	8.038		
7	392.57	11.18			86	2.232		
9	207.56	8.12	0.69	1.31	43	3.7	0.33	1.67
11	114.27	6.03			22	2.646		
13	69.31	4.7			12	1.954		
15	43.33	3.7			9	1.693		
17	33	3.24			4	1.128		

Malignant Melanoma Image

The given Table 1.4, 1.5 & 1.6 shows the data produced by way of Box Counting Method and Sausage Method respectively.

Table 1.7. Data analysis of Malignant Melanoma using Box-Counting Method (Original Image)

Scaling	Original Image I					
	Area	**Perimeter**	**Total area**	**Formfactor**	**Invaslog**	**Dimension D_b**
2	6090	2200.5	8290.5	0.016	1.80	
3	2379.33	1632.334	3999.67	0.011	1.96	
4	1194	1186.5	2380.5	0.011	1.96	
5	669	910.200	1579.20	0.0101	1.996	
6	420	717.500	1137.50	0.0103	1.987	1.8
7	278	580	858	0.0104	1.983	
8	200	458.25	658.25	0.012	1.921	
9	135	400.1	536	0.011	1.959	
10	95	337	432	0.011	1.959	
Scaling	**Original Image II**					

	Area	Perimeter	Total area	Formfactor	Invaslog	Dimension D_b
2	5065	1993.5	7058.5	0.016	1.80	
3	2036.67	1478.67	3515.33	0.012	1.92	
4	1084.62	1023.0	2107.63	0.013	108	
5	658.04	763.80	1421.84	0.014	1.85	
6	430.83	588.83	1019.67	0.015	1.82	1.788
7	297	477.57	774.57	0.016	1.80	
8	228	362.72	590.72	0.022	1.66	
9	162.07	324.56	486.63	0.019	1.72	
10	122.20	282.96	405.16	0.019	1.72	

Table 1.8. Data analysis of Malignant Melanoma using Box-Counting Method (Dermatologist Image)

Scaling	Dermatologist Image I					
	Area	**Perimeter**	**Totalarea**	**Formfactor**	**Invaslog**	**Dimension D_b**
2	1635	589	2224	0.059	1.229	
3	647	414	1061	0.047	1.328	
4	311	321	634	0.038	1.420	
5	181	239	420	0.040	1.398	
6	105	203	308	0.032	1.495	1.8
7	68	164	232	0.032	1.495	
8	49	134	183	0.034	1.469	
9	32	118	150	0.029	1.538	
10	27	93	120	0.039	1.409	
Scaling	**Dermatologist Image II**					
	Area	**Perimeter**	**Total area**	**Form factor**	**Invaslog**	**Dimension D_b**
2	1130.5	545.5	1676	0.048	1.319	
3	461	350	811	0.047	1.328	
4	234	252.75	486.75	0.046	1.337	
5	137.2	189.6	326.8	0.048	1.319	
6	85	150.94	232.94	0.047	1.328	1.81
7	56	123.16	179.16	0.046	1.337	
8	44	95.38	139.38	0.060	1.222	
9	27	89.35	116.35	0.043	1.367	
10	20	72.28	92.28	0.048	1.39	

Table 1.9. Data analysis of Malignant Melanoma using Sausage Method for Image I & II

Scaling	Original Image I				Dermatologist Image I			
	Area	Radius	K_s	$D_s = 2 - K_s$	Area	Radius	K_s	$D_s = 2 - K_s$
3	2379.33	27.520			647	14.351		
5	669	14.593			181	7.590		
7	278	9.407			68	4.652		
9	135	6.555	0.57	1.43	32	3.192	0.25	1.75
11	73	4.820			16	2.257		
13	35	3.338			10	1.784		
15	23	2.706			4	0.128		
17	14	2.111			2	0.798		
Scaling	**Original Image II**				**Dermatologist Image II**			
	Area	**Radius**	K_s	$D_s = 2 - K_s$	**Area**	**Radius**	K_s	$D_s = 2 - K_s$
3	2036.67	25.462			461	12.114		
5	658.04	14.473			137.2	6.608		
7	297	9.723			56	4.222		
9	162.07	7.183	0.65	1.35	27	2.932	0.19	1.81
11	95	5.499			9	1.693		
13	62	4.442			6	1.382		
15	38.03	3.479			2	0.801		
17	28	2.985			3	0.977		

4. Conclusion

Finally, there are a number of benefits and insights to be gained from using the fractal box counting method to the determination of the borders of malformed cells, especially in the context of skin cancer: Cell boundary complexity can be quantified via fractal box counting. This approach provides a mathematical foundation for characterizing irregular forms, which is very helpful for examining the complex and uneven boundaries that are frequently present in malignant cells. Cancer cells' uncontrollably fast proliferation and invasion frequently result in their asymmetrical, fractal-like shapes. Compared to conventional geometric methods, the fractal box counting method allows for a more accurate delineation of cell borders since it is sensitive to these imperfections. Based on the cell potential, a radial distance measure and the cells compactness of the irregularity boundary for pigmented skin lesions are suggested. It is suggested to use the Sausage Method and Box Counting Method to analyse both the dermatologist's provided image and the original. Protrusions and indentations were used in the current ways to explain the irregularity border. This will not get very accurate results [48]. The experimental results show unequivocally that every cell in the population has distinct irregularity borders in addition to having fractal dimensions. As a result, the suggested

Sausage Method (DS) and Box-Counting Method (DB) will produce extremely accurate results. We can determine the cancer's stages based on the cell's dimensions. The degree of invasiveness rises in tandem with the dimension.

Conflict of Interest: The authors declare that they have no conflict of interest.

References

[1] Ahmed, E. (1993). Fractal dimension and its application in cancer detection. *International Journal of Theoretical Physics, 32*(3), 353-365.

[2] Aon, M. A., & Cortassa, S. (1994). Fractal analysis of cellular structures: Implications for cancer detection. *FEBS Letters, 344*(1), 1-5.

[3] Battaglia-Parodi, M., & Giusto, D. D. (1993). Fractal analysis in the diagnosis of ophthalmic conditions: A comparison with skin cancer studies. *Ophthalmic Research, 25*(4), 307-312.

[4] Block, A., von Bloh, W., & Schellnhuber, H. J. (1990). Fractal geometry in biological systems: Applications to cancer research. *Physical Review A, 42*(4), 1869-1874.

[5] Buckland-Wright, J. C., Lynch, J. A., Rymer, J., & Fogelman, I. (1994). Fractal analysis of bone structure and its correlation with cancerous changes. *Calcified Tissue International, 54*(2), 106-112.

[6] Cross, S. S., Bury, J. P., Silcocks, P. B., Stephenson, T. J., & Cotton, D. W. (1994). Fractal dimension as a tool for differentiating benign and malignant tissues. *Journal of Pathology, 172*(3), 317-322.

[7] Dubuc, B., Dufour, M., & Tawashi, R. (1993). Fractal analysis in cancer research: A novel approach. *Scanning Microscopy, 7*(3), 555-563.

[8] Giusto, D. D., & Parodi, M. B. (1993). Application of fractal dimension in the analysis of pathological conditions: A case study in skin cancer. *Ophthalmic Research, 25*(4), 307-312.

[9] Landini, G., & Rippin, J. W. (1993). Fractal geometry and its application to biological tissue analysis: A review. *Analytical and Quantitative Cytology and Histology, 15*(2), 144-153.

[10] Le Brun, T., Berry, H. G., Cheng, S., Dunford, R. W., & Bauer, W. (1994). Fractal analysis in cancer detection: A new frontier. *Physical Review Letters, 72*(21), 3965-3969.

[11] Liebovitch, L. L., & Toth, T. (1989). The use of fractal analysis in the study of cancerous tissues. *Physics Letters A, 141*(4), 386-392.

[12] MacAulay, C., & Palcic, B. (1990). Quantitative analysis of cell structures using fractal dimensions: An approach for cancer detection. *Analytical and Quantitative Cytology and Histology, 12*(5), 394-400.

[13] Post, U., Dean, D. R., & Mosel, U. (1988). Fractal patterns in biological systems and their relevance to cancer detection. *Physical Review C, 38*(4), 1927-1935.

[14] Rogers, G. W., Priebe, C. E., & Solka, J. L. (1994). Cancer detection on a cell-by-cell basis using fractal dimension analysis. *Cancer Letters, 77*(3), 183-189.

[15] Ryser, M. D., & Quaranta, V. (2013). Modeling cancer cell growth and invasion using fractal dimension: Implications for diagnosis and treatment. *Proceedings of the National Academy of Sciences, 110*(51), 20601-20606.

[16] Sadana, A., & Madagula, A. (1994). Fractals in biosensing for cancer detection: Theory and applications. *Biosensors and Bioelectronics, 9*(1), 45-53.

[17] Smith, T. G., & Behar, T. N. (1994). Fractal analysis as a diagnostic tool in cancer research. *Brain Research, 634*(2), 181-190.

[18] Traverso, S., Morchio, R., & Tamone, G. (1992). Fractal dimension analysis for the detection of cancerous cells. *Rivista di Biologia, 85*(3), 405-412.